BMC Ecology and Evolution

RESEARCH

Open Access

Positive selection and relaxed purifying selection contribute to rapid evolution of sex-biased genes in green seaweed *Ulva*

Xiaojie Liu[1,2], Jonas Blomme[1,3,4], Kenny A. Bogaert[1], Sofie D'hondt[3], Emma Coulembier Vandelannoote[1,3,4], Thomas Wichard[5] and Olivier De Clerck[1*]

Abstract

Background The evolution of differences in gamete size and number between sexes is a cornerstone of sexual selection theories. The green macroalga *Ulva*, with incipient anisogamy and parthenogenetic gametes, provides a unique system to investigate theoretical predictions regarding the evolutionary pressures that drive the transition from isogamy to anisogamy, particularly in relation to gamete size differentiation and sexual selection. Its minimal gamete dimorphism and facultative parthenogenesis enable a rare window into early evolutionary steps toward anisogamy.

Results By analyzing the expression profiles of sex-biased genes (SBGs) during gametogenesis, we found that SBGs evolve faster than unbiased genes, driven by higher rates of non-synonymous substitution (d*N*), indicating that SBGs are under stronger selective pressures. Mating type minus-biased genes (*mt*-BGs) exhibit higher d*N*/d*S* values than mating type plus-biased genes (*mt*+BGs), suggesting stronger selective pressures on *mt*-BGs, although this difference was not statistically significant ($P = 0.08$). Using branch-site and RELAX models, we found positive selection and relaxed purifying selection acting on a significant proportion of SBGs, particularly those associated with flagella function.

Conclusions This study highlights the selective pressures shaping anisogamy and provides insights into the molecular mechanisms underlying its evolution. The faster evolution of SBGs, particularly *mt*-BGs, and the positive selection on genes associated with motility, such as those related to flagella function, suggest the importance of enhanced gamete motility in the transition to anisogamy. These findings contribute to our understanding of sexual selection and the evolutionary forces that drive the differentiation of gamete size and number between sexes.

Keywords *Ulva*, Anisogamy, Sexual selection, Sex-biased genes (SBGs), Positive selection, Relaxed purifying selection

*Correspondence:
Olivier De Clerck
Olivier.declerck@ugent.be
[1]Phycology Research Group, Center for Molecular Phylogenetics and Evolution, Ghent University, Ghent 9000, Belgium
[2]School of Marine Science and Engineering, Nanjing Normal University, Nanjing 210023, People's Republic of China
[3]Department of Plant Biotechnology and Bioinformatics, Ghent University, Ghent 9052, Belgium
[4]VIB Center for Plant Systems Biology, Ghent 9052, Belgium
[5]Institute for Inorganic and Analytical Chemistry, Jena School for Microbial Communication, Friedrich Schiller University Jena, Jena, Germany

Introduction

Sexual dimorphism, the phenotypic differentiation between males and females of the same species, is a widespread phenomenon in both animals and plants. In these organisms, sexual dimorphism is often reflected in significant differences in morphology, physiology and reproductive strategies. At the molecular level, dimorphism is associated with differential gene expression between the two sexes, referred to as sex-biased genes (SBGs), which are either located on autosomal or sex chromosomes [1, 2]. SBGs, especially those biased towards males, tend to exhibit rapid protein sequence evolution compared to unbiased genes, reflected by a higher ratio of non-synonymous (d*N*) to synonymous substitutions (d*S*) value [3–5].

The increased evolutionary rate of sex-biased genes can be attributed to sexual selection, related to differences in reproductive investment between males and females in terms of their contributions to offspring. Anisogamy imposes stronger sexual selection due to more intense gamete competition or gamete limitation in the sex with the smaller gametes [6]. However, empirical studies supporting this paradigm have primarily focused on organisms with pronounced sexual dimorphism and assumed conditions of negligible gamete limitation [7]. In contrast, sessile marine broadcast spawners often experience gamete limitation due to limited control over gamete dispersion and encounter rates [8]. Broadcast spawners include both isogamous and anisogamous organisms, including stages transitioning from isogamy to anisogamy, and could offer a broader understanding of reproductive strategies [9, 10]. Anisogamy has evolved several times independently in the evolution of eukaryotes from isogamy, which is frequently found in algae and produces two morphologically identical gametes (mating type plus, isogamy. The latter is *mt+* and mating type minus, *mt-*) [11].

Multiple theories describe possible selection pressures for the evolution of anisogamy. For instance, the pioneering theory considers the tradeoff between gamete size and number [12]; the ability of highly motile sperm to overcome sperm limitation for large immobile eggs [13, 14] and the adaptation for preventing nuclear–cytoplasmic conflict through uniparental inheritance of organelles [15]. The production of anisogamous gametes establishes the fundamental basis of maleness and femaleness [16]. According to the Darwin-Bateman paradigm, the evolution of anisogamy results in a reproductive asymmetry in which males, producing numerous small gametes, are subject to stronger selective pressure to invest in mating competition traits, while females, investing more resources in fewer large gametes, experience relatively lower selective pressure for such traits [6, 17]. The dynamics of gamete competition and gamete limitation, central to the "gamete dynamics" (GD) theory, may provide critical insights into the evolution of anisogamy in these systems. GD theory emphasizes the tradeoff between gamete size and number, suggesting that anisogamy can arise due to disruptive selection favoring small, mobile gametes for efficient fertilization and large, resource-rich gametes for zygote viability [10, 12, 14, 18, 19].

Brown algae such as *Ectocarpus* have been instrumental in testing these theories. Despite its morphologically isogamous gametes, *Ectocarpus* exhibits physiological anisogamy, with slightly larger female gametes that release pheromones to attract male gametes [20]. Analysis of SBGs in *Ectocarpus* revealed that both male- and female-biased genes exhibit faster evolutionary rates than unbiased genes, suggesting that both sexes experience selection pressures related to gamete function [20].

While the GD theory provides a compelling explanation for anisogamy, it also has limitations. For instance, some algae produce parthenogenetic gametes, which challenges the assumptions in GD theory that unfused gametes do not develop [21, 22]. Parthenogenesis reduces the selective pressure on traits enhancing gamete fusion efficiency, potentially favoring the evolution of smaller, isogamous, or slightly anisogamous gametes [21, 23]. Explaining this adaptation within GD theory requires considering how the absence of fusion impacts natural selection pressures and the evolutionary trajectories of gamete traits. This challenges key assumptions of GD theory, which often presumes that unfused gametes are a dead-end [21]. Empirical testing of these theoretical predictions is still limited, especially in systems with both near-isogamy and parthenogenetic potential.

Building on these theoretical frameworks and empirical studies, exploring model organisms that exhibit minimal gamete differentiation and parthenogenetic capabilities is essential. The green macroalgae of the genus *Ulva* are widely distributed in shallow marine and freshwater environments worldwide. Their isomorphic haplodiplontic life cycle has been well characterized, including a description of its two mating types: mating type minus (*mt-*) and plus (*mt+*), traditionally referred to as male and female, respectively. However, this assignment is not based on distinct morphological sexes but on slight differences in gamete size. Studies suggest that *Ulva* is isogamous to slightly anisogamous, with *mt+* gametes marginally larger than *mt-* gametes [24–27]. Ultrastructural studies have found few differences beyond the relative positions of the mating structure and eyespot [28, 29]. Contrary to *Ectocarpus*, where gametes are produced in specialized structures and exhibit distinct differences in motility and morphology, *Ulva* gametes are produced throughout the entire thallus and both gamete types are morphologically

similar [30]. This subtle dimorphism, along with *Ulva*'s ability to engage in parthenogenesis, makes *Ulva* a good subject to explore the subtle shifts from isogamy toward anisogamy [21, 22].

In this study, we conducted a time-course transcriptomic analysis of *U. mutabilis* gametogenesis, comparing expression patterns between *mt+* and *mt-* mating types. The results revealed (1) a statistically significant but biologically subtle difference in gamete size between *mt+* and *mt−* types,; (2) the identification of *mt+*BGs and *mt-*BGs during *Ulva* gametogenesis; (3) faster evolutionary rates of SBGs compared to unbiased genes (UBGs), with *mt-*BGs showing slightly higher rates than *mt+*BGs; and (4) positive and relaxed purifying selection on a subset of SBGs, particularly those related to flagellar function. These findings suggest that even in a near-isogamous, parthenogenetic species like *Ulva*, sexual selection and gamete motility may still exert evolutionary pressure, offering new insight into the early stages of anisogamy evolution.

Results

Low levels of sexual dimorphism in *Ulva*

The life cycle of *Ulva* consists of an alternation of isomorphic generations with morphologically identical *mt+* and *mt-* gametophytes (n) and sporophytes (2n). Meiosis occurs during the sporophyte generation, producing haploid zoospores that develop into either *mt+* or *mt-* gametophytes. Gametophytes produce either *mt+* or *mt-* gametes via mitosis. Gametogenesis involves a direct transformation of vegetative cells into biflagellated haploid gametes. *Ulva* gametes are traditionally described as morphologically and physiologically isogamous. Both *mt+* and *mt-* gametes exhibit motility and actively swim to encounter each other in the water column, pair and then spiral down to settle on the substrate. We used flow cytometry to measure the area of *mt+* and *mt-* gametes in *U. mutabilis* (Fig. S1). We found that *mt-* gametes were slightly smaller than *mt+* gametes, with a mean area of 19.75 and 21.72 μm², respectively ($n > 300$; Wilcoxon test, $P < 0.001$; Fig. 1B). The observed difference became statistically significant only after a substantial number of repetitions, implying that the sexual dimorphism in gamete size is subtle and requires a large sample size to be reliably detected.

Analysis of sex-biased gene expression during gametogenesis

To characterize SBGs expression during *Ulva* gametogenesis, the global gene expression of *U. mutabilis* as a function of time was characterized by RNA-sequencing. We sampled five time points: 0, 6, 24, 48 and 72 h after induction of gametogenesis of *mt+* and *mt-*, respectively, with three biological replicates for each time point and

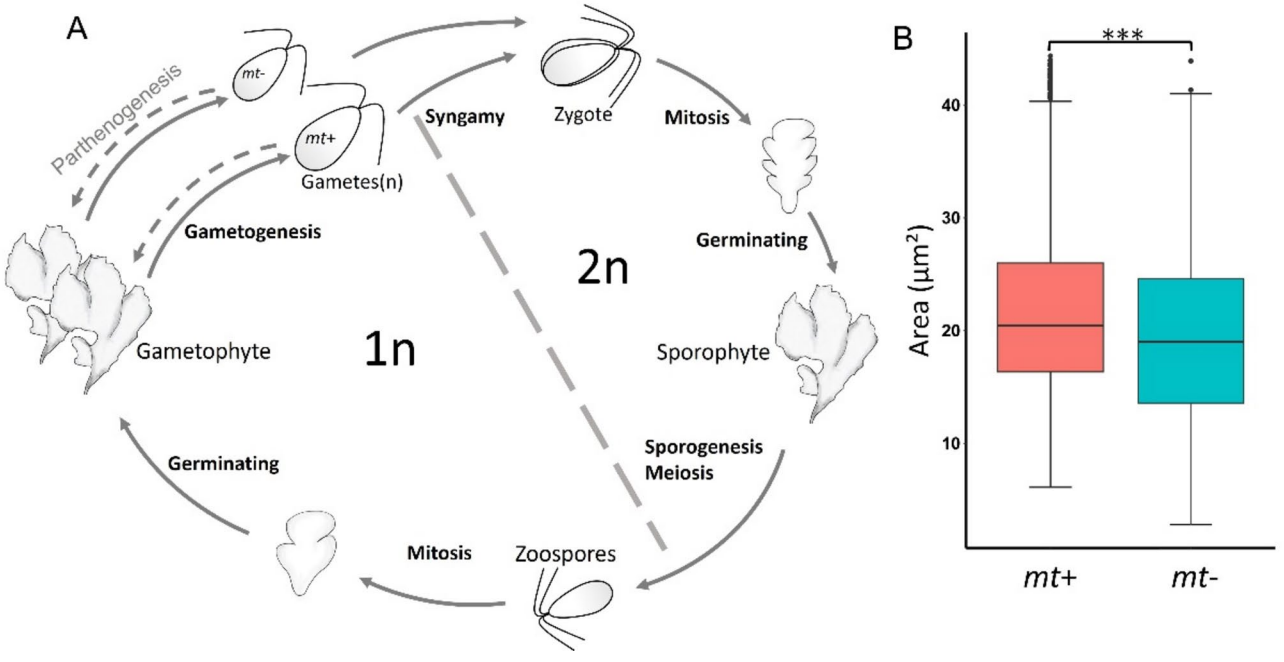

Fig. 1 The isomorphic life cycle of *Ulva*. **A**: The sexual life cycle of *Ulva* involves alternation between gametophytic and sporophytic life stages with identical morphologies. Sporophytes produce quadriflagellate meiotic spores (zoospores) that develop into haploid *mt+* or *mt-* gametophytes with similar morphology. Gametophytes produce *mt+* and *mt-* gametes by gametogenesis. Gametes of the opposite sex fuse in the water column to form a zygote (syngamy). Dashed arrows show the parthenogenetic development of gametophytes derived from unfused gametes. Zygotes develop to produce diploid sporophytes, completing the cycle. **B**: Boxplots of the area of *mt+* and *mt-* gametes of *U. mutabilis* derived from flow cytometry ($n = 307$ and 3170, respectively). The mean area of *mt-* gametes and *mt+* gametes are 19.75 and 21.72 μm², respectively ($P < 0.001$, Student's *t*-test).

strain. cDNA libraries were constructed with a QuantSeq™ 3' mRNA-Seq library prep kit (Lexogen) and a TruSeq RNA Sample Prep Kit (Illumina) for *mt+* and *mt-* strains. The 0 and 6 h represent the vegetative and determination phases, 24 and 48 h correspond to the differentiation phase, and 72 h marks the swarming phase [30]. RNA-sequencing resulted in 33×10^7 reads, with over 70% mapping to the *U.mutabilis mt+* genome. The mapped reads for each sample and the raw read counts for each gene are listed in Supplementary Tables S1 and S2.

We performed principal component analysis (PCA) of the transcriptomic data for the *mt+* and *mt-* samples separately (see Materials and methods; Fig. 2A and B) to visualize changes at the expression-level during the various stages of gametogenesis. PC1 captured 53.2% and 52.5% of the total variance for the time-course samples for *mt+* and *mt-*, respectively. The second and third PCs only capture 13.7% and 9.6% of the total variance, respectively. PC1 mainly reflects the previously described irreversible transition from a vegetative state to a reproductive state at 36 h (Fig. 2A and B; [31]). PC1 was, therefore, selected for further analysis. We performed a linear regression analysis based on the gene contributions to PC1 of *mt+* and *mt-*. The gene contributions to PC1 of *mt+* and *mt-* fit a linear regression model and the genes with high residuals in the model were interpreted as SBGs during *Ulva* gametogenesis (Fig. 2C). Using a threshold of residuals greater than 0.01 or smaller than −0.01, similar to the 90% prediction interval of the linear model, we identified 377 *mt+*BGs and 320 *mt-*BGs during gametogenesis (Fig. 2C Supplementary Table S3).

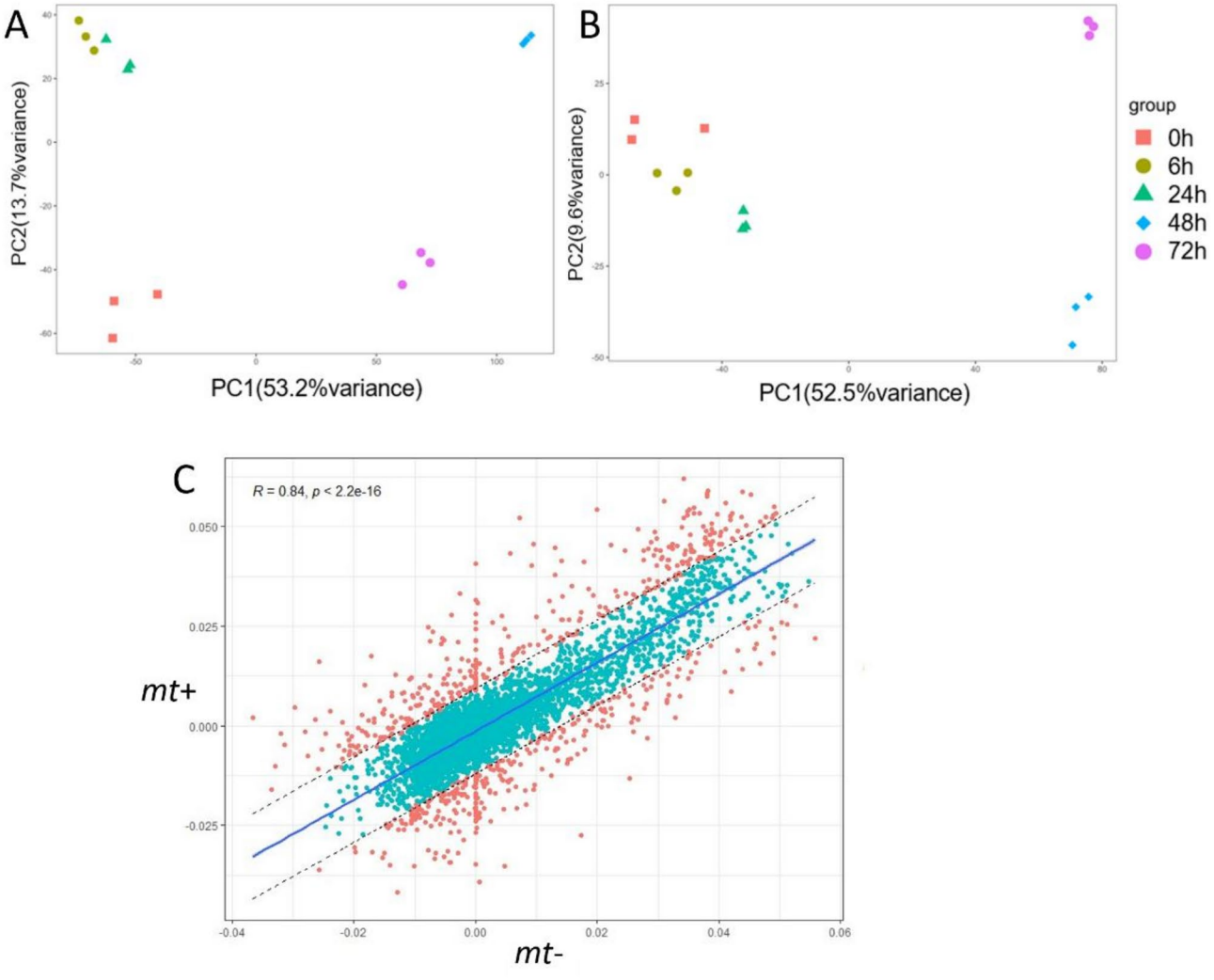

Fig. 2 PCA plots for *mt+* **(A)** and *mt-* **(B)** transcriptomes during gametogenesis. Biological replicates ($n = 3$) are indicated with the same color and shape. **C**: Linear regression analysis of gene contribution to PC1 variation during *Ulva* gametogenesis ($P < 0.001$). The x-axis represents the gene contribution to PC1 variation of *mt-* and the y-axis represents the gene contribution to PC1 variation of *mt+*. Outlier genes with residuals bigger than 0.01 are indicated with red color and are considered SBGs during *Ulva* gametogenesis. The dashed lines indicate the 90% prediction interval of the linear model.

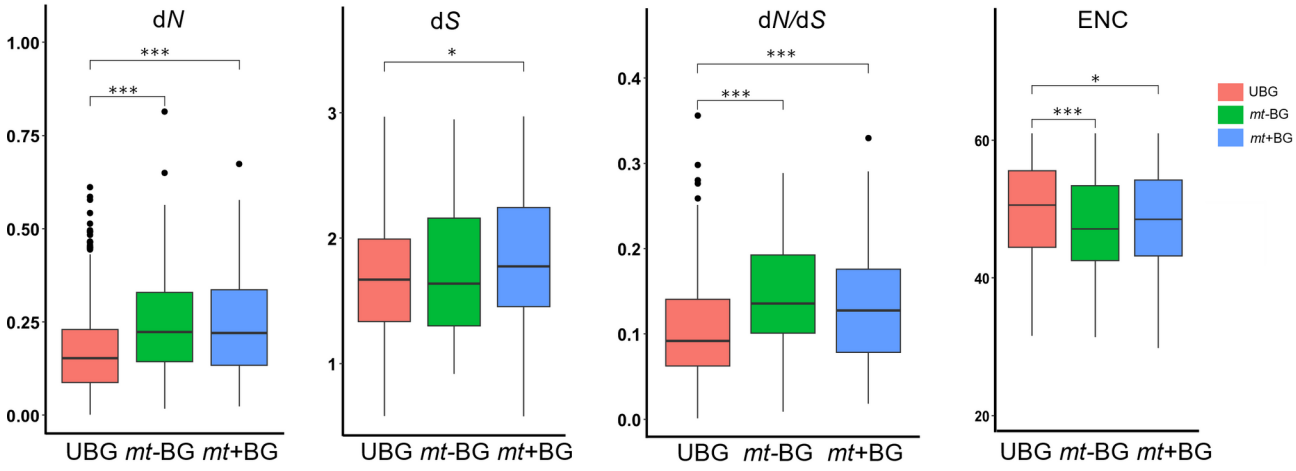

Fig. 3 Rates of evolution and ENC of unbiased (UBG), mating type minus-biased (*mt*-BG) and mating type plus-biased (*mt*+BG) genes during gametogenesis. Overall d*N*, d*S*, and d*N*/d*S* ratios were calculated by comparing orthologous gene sequences from *U. mutabilis* and *U. prolifera* by CODEML. d*N*: nonsynonymous substitutions, d*S*: synonymous substitutions, d*N*/d*S*: ratio of nonsynonymous to synonymous substitutions, ENC: effective number of codons. Pairwise statistical significance between the two groups of SBG and UBG was calculated by Wilcoxon test, statistically significant differences are indicated (**P* < 0.05, ***P* < 0.01, ****P* < 0.001).

Sex-biased genes evolve more rapidly than unbiased genes

To test for differences in rates of evolutionary divergence between SBGs and UBGs, we calculated levels of pairwise non-synonymous (d*N*) and synonymous (d*S*) substitutions between *U. mutabilis* and *U. prolifera*. The UBGs were defined as those fitting the linear model well (Fig. 2C) and we randomly selected 697 genes for further analysis.

We identified 105, 182 and 532 one-to-one orthologous groups (OGs) between *U. mutabilis* and *U. prolifera* out of 320 *mt*-BGs, 377 *mt*+BGs and 697 UBGs respectively. Both *mt*-BGs and *mt*+BGs have a lower percentage of one-to-one OGs compared to UBGs (Wilcoxon test, $P < 0.001$). In addition, *mt*-BGs have a lower percentage of one-to-one OGs compared to *mt*+BGs (Wilcoxon test, $P < 0.001$).

To test for differences in rates of evolutionary divergence between different categories of SBGs and UBGs, we calculated levels of nonsynonymous (d*N*) and synonymous (d*S*) substitution using pairwise comparisons with orthologs from *U. prolifera*. We found that both *mt*-BGs and *mt*+BGs have significantly higher d*N*/d*S* values compared to UBGs (Wilcoxon test, $P < 0.001$; Fig. 3), which suggests that SBGs evolve more rapidly than UBGs and that stronger evolutionary pressures act on these genes. The elevated d*N*/d*S* values for SBGs compared with unbiased genes were due to significantly higher levels of non-synonymous substitution (Wilcoxon test, $P < 0.001$; Fig. 3). A higher d*N*/d*S* ratio in SBGs indicates that these genes are subject to positive selection or relaxed purifying selection. We found the d*N*/d*S* values of *mt*-BGs ($n = 79$) are slightly higher than *mt*+BGs ($n = 141$), with values of 0.18 and 0.16, respectively. However, the difference is not statistically significant (Wilcoxon test, $P = 0.08$). Additionally, both *mt*-BGs and *mt*+BGs exhibit significantly lower Effective Number of Codons (ENC) values than UBGs (Wilcoxon test, $P < 0.001$). Higher codon usage bias likely reflects the functional importance and translational efficiency of these genes in sex-specific contexts. Overall, the elevated d*N* and d*N*/d*S* values for SBGs suggest stronger selective pressures on these genes due to their roles in sexual reproduction and sex-specific traits, while the lower ENC values point to a higher degree of codon usage bias.

We further tested whether the differences in d*N*/d*S* values were due to positive selection. Utilizing annotated *U. compressa*, *U. prolifera* and *U. mutabilis* genomes supplemented with a high-quality transcriptome assembly of *U. linza*, we performed a phylogenetic analysis to detect positive selection. We tested the SBGs and UBGs using the paired nested site models (M1a, M2a; M7, M8) implemented in PAML4 (CODEML) [32]. The second model in each pair (M2a and M8) is derived from the first by allowing variable d*N*/d*S* values between sites to be bigger than one, making it possible to detect positive selection. This analysis detected 21 SBGs out of 102 (21%) under positive selection based on either one or both pairs of models (M1a-M2a, M7-M8; LTRs, Wilcoxon test, $P < 0.05$; Supplementary Table S4). A slightly lower percentage of UBGs were under positive selection (18%; 51 out of 285 OGs), but this difference was not statistically significant (Wilcoxon test, $P = 0.56$). These results suggest that a subset of *S*BGs is evolving under adaptive pressures, potentially linked to gamete function or reproductive roles.

Selective pressure for sex-biased genes

To investigate whether the SBGs during gametogenesis in *Ulva* undergo positive selection in the anisogamous branch, we selected three isogamous species belonging to the Chlorophyceae (*Chlamydomonas reinhardtii*, *Astrephomene gubernaculifera* and *Gonium pectorale* [33]) as background branch and three *Ulva* species (*U. compressa*, *U. mutabilis*, *U. prolifera*) as foreground branch to perform positive selection analysis under a branch-site model. We then identified 1,928 one-to-one OGs among six species and established a species phylogeny as: (((*U. compressa*, *U. mutabilis*), *U. prolifera*), (*C. reinhardtii*, (*A. gubernaculifera*, *G. pectorale*))). Among these, 43 OGs were found within the SBGs identified during *Ulva* gametogenesis.

The analysis revealed positive selection affecting specific amino acid sites along the predefined foreground anisogamous branches, where d*N*/d*S* ratio varies among lineages and across sites [32]. Upon comparing the A model (model = 2, NSsites = 2, allowing $\omega > 1$ on the foreground branch) and null model (identical except with ω fixed = 1 on the foreground), we discovered that 14 out of 43 (33%) exhibited strong evidence of having specific sites that evolved under positive selection based on the d*N*/d*S* value for the foreground branch of *Ulva* lineage (Supplementary Table S5). Further investigation using Phytozome revealed that 6 of these 14 genes under positive selection are associated with flagella, with top hits of orthologous comparisons to known flagella-related genes of *C. reinhardtii*. This finding suggests that motility-related functions may be under adaptive pressure during gamete evolution in *Ulva*.

To complement the branch-site test, we also applied the RELAX model to assess selection intensity. We found that 13 out of 43 OGs ($k = 0.08$-0.79, $P < 0.05$, Supplementary Table S6) experienced relaxed purifying selection. Among these, four genes were identified as flagella-associated based on ortholog searches against *C. reinhardtii*.

Discussion

The green macroalgae of *Ulva*, a species capable of parthenogenesis, produces female (*mt+*) and male (*mt-*) gametes of slightly different sizes from morphologically identical gametophytes through gametogenesis. *Ulva* reproduces via broadcast fertilization, releasing gametes into the water where external fertilization occurs without parental care - conditions that align closely with the key assumptions of the widely accepted GD model [34]. However, *Ulva* gametes can also develop without fertilization, parthenogenesis [35], diverging from GD model assumptions that rely on fertilization for gamete success. Although recent theoretical extensions of the GD model have begun to incorporate parthenogenetic gametes, few empirical studies have tested these additions [21, 23]. Anisogamy is often thought to promote mating competition among males. The release of gametes in the water column possibly leads to gamete limitation and reduces the probability of successful fertilization, which limits the availability of gametes for fertilization rather than creating direct competition between sexes [6]. This unique combination of traits makes *Ulva* an interesting model for testing theories of anisogamy evolution, including both the GD model and the Darwin-Bateman paradigm [21, 22]. However, other physiological constraints contribute to gamete success. Due to their strong phototaxis, gametes of both mating types are attracted to light, particularly the brightest spot. This behavior is thought to optimize their chances of mating and survival. The congregation of gametes in a well-lit area reduces the distance they must swim to find each other, increasing the probability of successful mating. Overall, this phototactic behavior is an adaptive strategy that improves reproductive efficiency in *Ulva*, ensuring successful gamete fusion and propagation of the species. As discharged gametes often show batch-dependent fitness indicated by their swarming speed [36], fast swarmers can out-compete the slower ones.

In this study, we demonstrated that *Ulvamutabilis* exhibits slight anisogamy, with *mt+* gametes being slightly larger than *mt-* gametes. The mean areas of *mt+* and *mt-* gametes are 21.72 and 19.75 μm^2, respectively, indicating that *Ulva* produces relatively small gametes. Previous studies on *U. prolifera* have reported that female gametes typically measure around 6.7 μm in length and 4.1 μm in width, while male gametes average about 6 μm in length and 3.4 μm in width [37]. Despite being statistically significant, this size difference is subtle and likely represents incipient anisogamy. Notably, *Ulva* has been cultured as single-sex populations for several decades until today [38, 39]. *Ulva* inhabits shallow waters in the upper intertidal zone and has evolved mechanisms for synchronous gamete release during daytime at low tides. The gametes display positive phototaxis, moving toward light to increase the likelihood of encounters just beneath the two-dimensional sea surface, thereby maximizing fusion opportunities. Consequently, *Ulva* may not experience strong gamete limitation, resulting in a small, slightly anisogamous gamete system that aligns well with the predictions of the newly developed GD model [21].

Gametogenesis of *Ulva* encompasses a determination phase, a differentiation phase and a swarming phase, which takes 72 h to complete [31, 40]. We sampled five time points: 0, 6, 24, 48, and 72 h for transcriptome sequencing. The 0 and 6 h represent the vegetative phase and the determination phase, 24 and 48 h covers the differentiation phase, and 72 h mark the swarming phase. Since 36 h post-induction is a critical checkpoint where blade cells commit irreversibly to gametangium

differentiation, we included two samples within this phase [31]. We used two different library preparations for *slender* (*mt+*) (TruSeq RNA Sample Prep Kit) and wild-type (*mt-*) (Quantseq™ 3' mRNA-Seq library prep kit) gametogenesis. The Quantseq™ mainly generates reads mapped towards the 3′ end of CDS and the 3′UTR, which induces a batch effect, rendering traditional differential expression analysis unsuitable for direct comparison across time points. Additionally, measuring expression levels irrespective of time points does not provide information about the dynamic interactions that characterize the cellular processes, which is our focus. Hence, we applied a PCA-based method to identify sex-biased genes for our time-course study, as outlined by Jonnalagadda and Srinivasan [41]. The contribution of a gene to a principal component (PC) is the correlation between the gene and the PC. Comparing the scores is equivalent to comparing the similarity of temporal expression profiles. Using the dominant PCs minimizes noise, including potential induction efficiency differences between mating types and batch effects from sequencing methods, facilitating meaningful expression profile comparisons. This leads to the meaningful comparison of expression profiles across conditions and identifies significant differentially expressed genes in the time course study [41]. In our study, PC1 captured more than 50% of the total variance, captured systematic changes in expression. Using linear regression model, we identified 697 sex-biased genes during gametogenesis, accounting for ~ 10% of the total analyzed genes. The result is in accordance with the analysis in *Ectocarpus*, in which, less than 12% of the genes were found to be differentially regulated between sexes [20].

Our analysis revealed that SBGs exhibit significantly fewer one-to-one orthologous groups (OGs) compared to UBGs, and that *mt*-BGs have significantly fewer one-to-one OGs compared to *mt* +BGs. This suggests that *mt*-BGs have undergone more frequent gene duplication or loss events than *mt*+BGs, implying that SBGs, particularly *mt*-BGs, may experience faster and more dynamic evolutionary changes. This elevated rate of gene turnover in *mt*-BGs compared to *mt* +BGs may reflect unique selective pressures acting on *mt*-BGs, potentially driven by sexual selection or competition. The frequent gene duplication and loss events observed in SBGs support the idea that duplication promotes functional divergence and phenotypic innovation, as it reduces the constraints of purifying selection on the newly duplicated gene, allowing it to acquire new functions over time [42].

We show that both *mt-* and *mt+* biased genes in gametogenesis exhibit faster evolutionary rates (higher d*N*/d*S*) compared to unbiased genes, consistent with findings in *Ectocarpus* [20]. The rapid evolutionary rates of sex-biased genes are believed to be partly driven by positive selection, with sexual selection and/or sexual antagonism as the likely underlying factors [6, 17]. For *Ulva*, our analysis indicated that the d*N*/d*S* ratio for *mt*-BGs was slightly higher than that of *mt*+BGs. Given the proximity to conventional thresholds for significance, it may warrant further investigation into potential selective pressures acting differently on *mt*-BGs and *mt*+BGs. The most straightforward explanation, which aligns with the low levels of sexual dimorphism in this system, is that both *mt-* and *mt+* are under sexual selection. *mt-* and *mt+* gametes are small, motile cells produced in large quantities in plurilocular gametangia and they are released to the brackish waters [40, 43]. The synchronous release of gametes, stimulated by low tides, along with the positive phototactic behavior of the gametes, facilitates effective fusion [40]. Consequently, the system is not strongly limited by gamete availability, and both sexes may experience competitive conditions for fertilization in nature. However, the intensity of this competition may not be sufficient for males to exhibit a significantly higher evolutionary rate compared to females. Taken together, our results indicate that both *mt-* and *mt+* are under sexual selection in slight anisogamous *Ulva*, in line with the recent developed models that both *mt-* and *mt+* can be under competition except under high gamete density [8].

Higher d*N*/d*S* ratios in SBGs can be attributed to several factors, including positive selection, relaxation of purifying selection, or codon usage bias [1]. Previous studies have suggested that genes exhibiting sex-biased expression and rapid evolutionary rates generally tend to have lower codon usage bias compared to unbiased genes [33]. However, our findings contrast with this trend, as we observed that SBGs had significantly lower effective numbers of codons (ENC) compared to UBGs, suggesting stronger codon usage bias in SBGs (Fig. 3). Additionally, if the higher d*N*/d*S* ratios in SBGs were due to codon usage bias, we would expect lower d*S* rates in SBGs compared to UBGs, because selective constraints at synonymous sites would reduce synonymous codon replacements [44]. However, we observed that d*S* values for *mt*+BGs were higher than UBGs, while there was no significant difference between *mt-* and *mt+*, indicating that rapid evolutionary rates in SBGs are not associated with reduced codon usage bias. Instead, we found large percentage (21%) of SBGs are under positive selection using F3 × 4 model of codon frequencies among *Ulva* linages.

Both sexual selection and sexual antagonism—especially in the context of gamete recognition, where interactions between surface proteins on sperm and egg cells determine fertilization success—are likely major drivers of the rapid evolution observed in many sex-biased genes involved in reproduction [45]. We were able to detect instances of positive selection and relaxed purifying selection affecting specific branch or amino acid site [32,

46, 47]. The branch-site model analysis revealed that 14 out of 43 SBGs (33%) exhibited strong evidence of positive selection, specifically within the anisogamous *Ulva lineage*. Relaxed selection may occur when the efficiency of natural selection is dramatically reduced or eliminated at either the gene or genome-wide level, leading to accumulations of deleterious mutations with respect to positive selection. This has been proposed as an explanation for the rapid evolution of sex-biased genes [48]. Our analysis using the RELAX model identified 13 out of 43 SBGs as experiencing relaxed purifying selection. Relaxed selection can lead to an accumulation of deleterious mutations and may explain the rapid evolution observed in SBGs [49]. The observed higher d*N*/d*S* ratios in SBGs, coupled with evidence of both positive and relaxed selection, indicate that SBGs are subject to complex evolutionary forces. Positive selection likely drives the rapid adaptation of these genes to enhance reproductive efficiency and success, while relaxed selection allows for variation and experimentation in gene function, contributing to the diversity and evolution of reproductive strategies [34, 50].

Intriguingly, among these genes, we found that 6 out of 14 and 4 out of 13 genes under positive selection and under relaxed purifying selection, respectively, are orthologs of genes coding for flagella associated proteins in *C. reinhardtii*. Flagella-mediated gamete recognition is a fundamental aspect of fertilization and the initial contact between mating gametes is made by flagella [28]. However, the fate of the flagella after fertilization differs between *Chlamydomonas* and *Ulva*. In *Chlamydomonas*, the flagella are detached from the zygote, whereas in *Ulva*, all four flagella are absorbed into the zygote [28, 51]. Interestingly, in *Fucus*, 3 of the 21 male-biased genes under positive selection were associated with the sperm flagella [52]. The identification of flagella-associated genes under positive selection highlights the potential importance of motility and gamete interaction in the evolutionary process. Positive selection on these genes may enhance the motility and efficiency of sperm, thereby increasing fertilization success and supporting the transition from isogamy to anisogamy. This observation aligns with the theories proposing evolutionary advantages conferred by enhanced sperm motility [13, 14]. The theory emphasizes adaptations that enhance sperm motility as a critical factor in reproductive success. The presence of flagella-associated genes among those under relaxed selection suggests that while some aspects of flagellar function are under strong selective pressure, others may be less constrained, allowing for variation and divergence in gene function.

In summary, our study demonstrates that *U. mutabilis*, a parthenogenetic and near-isogamous species, exhibits slight gamete size dimorphism and significant divergence in mating type-biased gene evolution. Both *mt*+BGs and *mt*-BGs evolve faster than unbiased genes, driven by positive selection and relaxed purifying selection. Notably, many of these rapidly evolving genes are related to flagellar function, underscoring the adaptive importance of motility and gamete interaction in reproductive success. These results support the expansion of gamete dynamics theory to include parthenogenetic systems, and they provide empirical evidence for how subtle anisogamy can still generate strong evolutionary pressures. *Ulva* thus serves as a powerful model for studying the earliest transitions toward anisogamy and sexual dimorphism. Future work should explore broader sampling of *Ulva* genotypes and other near-isogamous species to test the generality of these findings, particularly regarding the evolutionary fate of motility genes and the balance between selection types across mating types.

Materials and methods

Strains and culture conditions

Haploid gametophytes of *Ulva mutabilis* belonging to both mating types [strain "wild-type" (*mt*-) (FSU-UM1-41) and "*slender*" (*mt*+) (FSU-UM5-1)] used for this study were obtained from Friedrich Schiller University Jena and originally collected by Føyn (1958) in southern Portugal. Zygotes can be easily generated from *mt*- and *mt*+ gametes, which develop into normal *mt*- / *mt*+ sporophytes producing zoids of both mating types by meiosis [39]. We determined the mating types of the two strains by identifying the mating type locus through whole genome sequencing (unpublished data) and compared it with the published *U. partita* sex locus sequence [53]. Gametophytes of *Ulva* were raised parthenogenetically from unmated gametes and cultured in culture vessels containing 2 L Provasoli enriched seawater (PES) medium [54] with the following specific parameters: light intensity, 70 μmol photons·m^{-2}·s^{-1}; temperature, 18 ± 1 °C; and 17:7 h light: dark cycle. The medium was completely changed every 2 weeks until the algae were fertile (~ 10 weeks). Afterwards, the medium was partially (20%) changed every week to avoid induction of gametogenesis.

Induction of gametogenesis

Intact mature thalli of *Ulva mt*+ and *mt*- strains were cut into 1–3 mm^2 fragments using an herb chopper. Fragments were washed 3 times for 15 min with autoclaved seawater to remove sporulation inhibitors [40, 55] and transferred to a new culture medium to induce gametogenesis. Fragmented thalli were sampled at 0, 6, 24, 48 and 72 h following the induction of gametogenesis [31]. Samples were flash-frozen in liquid nitrogen and stored at -80 °C.

Measurement of gamete size

The culture medium was refreshed and the swarming gametes were concentrated by positive phototaxis using a unidirectional light source after 72 h induction. Gametes were collected in Eppendorf tubes and the number and sizes were measured using flow cytometry (ImagestreamX MkII, Cytek), and using the IDEAS™ analysis software (Amnis-Millipore-Sigma, USA) to extract the area of the gametes.

RNA extraction and RNA sequencing

Total RNA was extracted using a CTAB method [56]. The quality and quantity of total RNA was evaluated with a NanoDrop™ 2000c spectrophotometer (Thermo Fisher Scientific) and Bioanalyzer RNA6000 (Agilent Technologies). For wild-type (*mt-*) strain, cDNA libraries were constructed with a Quantseq™ 3' mRNA-Seq library prep kit (Lexogen) following the manufacturer's instructions. For *mt+*, the sequence libraries were constructed with a TruSeq RNA Sample Prep Kit (Illumina) according to the manufacturer's protocol. Illumina sequencing was performed using the Illumina Nextseq 500 platform to produce 150 bp single-end reads. RNA-seq reads generated for *mt+* and *mt-* gametogenesis are available with accession number PRJNA1212590 and PRJNA773495 respectively. Reads were mapped to the *Ulva mt+* genome version (available at https://bioinformatics.psb.ugent.be/orcae/overview/UlvmuSL, unpublished) that contain annotated untranslated regions (UTRs), contrary to the published *Ulva* wild-type genome [57],. The UTR of the *mt+* genes was annotated by PASA (https://github.com/PASApipeline/PASApipeline/wiki) based on the RNAseq data generated during the gametogenesis of *U. mutabilis* [30, 58]. Reads were mapped using TopHat ver. 2.1.1 [59] with default parameters. The number of mapped reads was calculated using HTseq [60] and read numbers were normalized by the R package *edgeR* [61].

Identification of the sex-biased genes during gametogenesis

Out of 13,323 genes in the annotated *mt+* genome, we annotated 6,767 genes with UTR and selected these for further analysis to mitigate the coverage difference between the two library preparations. Due to the distinct mapping of reads, direct comparison of read numbers between the *mt+* and *mt-* using common packages like EdgeR and DEseq was not feasible. To address this issue, we conducted PCA based differential gene expression analysis.

To identify the differential expressed genes during the dynamic process of gametogenesis, we performed principal component (PCA) based analysis [41]. First, we performed PCA analysis for the *mt+* and *mt-* gene expression data during gametogenesis (0, 6, 24, 48, 72 h after induction) separately. We calculated the gene contributions to the principal components by R v4.0.4 to capture most of the variance between the vegetative phenotype and the reproductive phenotype for the *mt-* and *mt+* respectively. Next, we performed regression analysis based on the contribution values of each gene to the principal components capturing most of the variance. We calculated the residuals of each gene to the regression linear model. The dispersed genes with residuals bigger than 0.01 (similar as the threshold of the 90% prediction interval) from the regression model were identified as sex-biased genes in *Ulva* gametogenesis.

Measurement of synonymous and nonsynonymous substitution rates

The genome sequence of *U. compressa* (GCA_024500015.1) and *U. prolifera* (GCA_023078555.1) were retrieved from NCBI database. Genome annotation followed a series of steps: Initially, a de novo repeat identification was performed with RepeatModeler [62]. Unknown elements were screened with BLASTX (E-value < 1e-5) against UniRef91 database (Suzek et al. 2014) (subset Viridiplantae) and removed from the repeat library if necessary. The filtered *Ulva* repeat library was applied by RepeatMasker (4.0.7) [63] to mask the repetitive elements in the assembly. Afterwards, we applied EvidenceModeler [64] to predict gene models. The consensus gene models were reconciled using the models from ab initio and orthology-aided predictions, transcripts reconstructed from RNA-Seq, and homologous models derived from the protein alignments of the available public resource. We used BRAKER1 v1.9 [65] to predict the gene models incorporating the RNA-Seq mapping results generated using Stringtie2 [66]. We further used Augustus v3.2.3 with the trained data from BRAKER1 and the protein profile extension to re-predict the gene models [67]. In addition to the ab initio prediction, the RNA-Seq data were also used to reconstruct the transcripts, which consisted of consensus transcripts predicted by Scallop v0.10.2 [68] and predicted coding regions of Trinity v2.4.0 assemblies (both *de novo* and genome-guided) using PASA [64]. Finally, 13,405 and 12,983 genes were annotated for *U. compressa* and *U. prolifera* genome, respectively. Published transcriptome data of *U. linza* [69] were downloaded and one-to-one orthologs were identified using OrthoFinder v2.5.5 with default parameters for the genomes of *Ulva*, *U. compressa*, *U. prolifera* and transcriptome assembly of *U. linza* [70].

Unbiased genes were a random subset of 697 genes which fit the linear regression model well in the regression analysis between slender (*mt+*) and wildtype (*mt-*). Putative orthologs between *U. mutabilis* and *U. prolifera* were aligned using Muscle embedded in TranslatorX

[71], generating a codon-to-codon alignment. The alignment was transformed to PAML4 format using PAL2NAL script (https://github.com/liaochenlanruo/PAL2NAL). Sequences with gapless alignments exceeding 100 base pairs were retained for pairwise d*N*/d*S* analysis. This analysis was performed using the Phylogenetic Analysis by Maximum Likelihood (PAML) software, specifically the CODEML program with the F3 × 4 model which estimates codon frequencies from the nucleotide frequencies at the three codon positions, and runmode set to 2, as implemented in the PAL2NAL suite [72]. For the positive selection test, codon-to-codon alignments among *U. mutabilis*, *U. compressa*, *U. prolifera* and *U. linza* were obtained as described above. CODEML paired nested site models (M0; M1a, M2a; M7, M8) [32, 73] of sequence evolution were used and the outputs were compared using the likelihood ratio test. Bayes Empirical Bayes (BEB) methods allowed for identification of positively selected sites a posteriori. Genes with saturated synonymous substitution values (d*S* > 3) were excluded from the analysis.

The ENC values were calculated for all SBGs and UBGs in the study using CAIcal server (http://genomes.urv.es/CAIcal/)(Kumar et al. 2018). Lower ENC values signify stronger codon usage bias. We performed a Wilcoxon test to determine if there are deviations in ENC values between SBGs and UBGs.

Estimation of strength of natural selection

To estimate the natural selection strength from isogamy to slight anisogamy for the sex-biased genes, we downloaded published isogamous genome datasets *Astrephomene gubernaculifera* (GCA_021605115.1), *Chlamydomonas reinhardtii* (GCF_000002595.2) and *Gonium pectoral* (GCA_001584585.1) in Chlorophyceae, which have closer phylogenetic relationship with *Ulva* genus. Afterwards, we identified one-to-one orthologs using OrthoFinder v2.5.5 with default parameters for these three genomes and the three *Ulva* genomes described above. Then we conducted separate analyses using classical branch-site model and in PAML package [32] and he RELAX model in HYPHY v2.5 [46, 47] to distinguish which evolutionary forces are driving the rapid evolutionary rates of SBGs.

To determine if amino acid sites in the foreground have undergone positive selection compared with the background for each OGs, we followed the protocols of Alvarez-Carretero et al. (2023). We used branch-site model A (model = 2, Nssites = 2, fix_omega = 0, omega = 0.5) and null model (model = 2, Nssites = 2, fix_omega = 1, omega = 1). We set up the *Ulva* linage as foreground branch. We examined the significance of likelihood ratio tests (LTRs, $P < 0.05$) to identify positively selected sites between model A and null model by comparing LRTs to the Chi-square distribution with one degree of freedom. The homologs and functional annotation of the genes identified under positive selection were obtained from Phytozome (https://phytozome.jgi.doe.gov/pz/portal.html).

To test the relaxation of selective strength, we used the RELAX model in the HyPhy v2.5 software (Kosakovsky Pond et al. 2020; Wertheim et al. 2015). The RELAX model determines the proportion of sites in the test (foreground) and reference (background) branches using a branch-site model. Essentially, RELAX estimates three ω (d*N*/d*S*) parameters ($\omega 0 \le \omega 1 \le 1 \le \omega 2$). The first two ω classifications indicate that sites have undergone purifying selection and the third classification indicates that sites have been under positive selection. Subsequently, the model introduces a selection intensity parameter (K value) to compare a null model (K = 1) with an alternative model, thereby assessing the strength of natural selection. When K < 1, indicates relaxed purifying selection in the test branch relative to the reference branch. We quantified the statistical confidence of K value ($P < 0.05$) using LRTs.

Supplementary Information

The online version contains supplementary material available at https://doi.org/10.1186/s12862-025-02382-y.

Supplementary Material 1: Table S1-S5 are listed in Supplementary_materials.xlsx. Table S1: The total number of mapped reads for each sample. Table S2: The raw reads count mapped for each gene. Table S3: ***mt-***BGs, ***mt+***BGs and UBGs list. Table S4: Positive selection evidence of SBGs. Table S5: Evidence of positive selection using Branch-site model. Table S6: Evidence of relaxed purifying selection using RELAX model.

Supplementary Material 2: Figure S1: Comparison of gamete size distribution between ***mt+*** and ***mt-*** of ***U. mutabilis***. Representative images of individual gametes from the ***mt+*** (A) and ***mt-*** (B) populations captured under brightfield (Ch01), GFP fluorescence (Ch02), and merged GFP/RFP (Ch06) channels at 60 × magnification. Scale bar = 7 µm; C: Normalized frequency distribution of gamete sizes for ***mt+*** (orange line) and ***mt-*** (red line) populations.

Acknowledgements

Not applicable.

Author contributions

X.L., and O.D.C. designed the study. X.L., T.W., E.C.V. and S.D. performed experiments. X.L., J.B. and K.B. performed the transcriptional analysis. X.L. wrote the manuscript with contributions from all authors.

Funding

Funding for this research was provided by FWO Research Grant (G015623N) to O.D.C. This work makes use of resources and facilities provided by UGent as part of the Belgian contribution to EMBRC-ERIC (FWO I001621N) and the Betty Moore Foundation for a SYMBIOSIS grant (nr. 4546891618). X.L. is indebted to the China Scholarship Council (201504910698) and Ghent University Special Research Fund (BOF-16/CHN/023) for a PhD grant and to COST Action FA1406 (Phycomorph) for a Short-Term Scientific Mission to Friedrich Schiller University Jena. J.B. thanks the Research Foundation – Flanders (FWO) for a postdoctoral fellowship (12T3418N) and Ghent University Special Research Grant (BOF20/PDO/016). T.W. was funded by the Deutsche Forschungsgemeinschaft through Grant No. SFB 1127/2 ChemBioSys–239748522.

Data availability
Sequence data that support the findings of this study have been deposited in the NCBI with the primary accession code PRJNA1212590 and PRJNA773495. The raw reads of ***mt+*** genome of ***U. mutabilis*** are accessible under BioProject number PRJEB25750 and the assembled genome sequence and annotation of the genome is available via the Online Resource for Community Annotation of Eukaryotes (ORCAE) at https://bioinformatics.psb.ugent.be/orcae/overview/UlvmuSL.

Declarations

Ethics approval and consent to participate
Not applicable.

Consent for publication
Not applicable.

Competing interests
The authors declare no competing interests.

Received: 16 January 2025 / Accepted: 25 April 2025
Published online: 09 May 2025

References

1. Zhang Z, Hambuch TM, Parsch J. Molecular evolution of sex-biased genes in *Drosophila*. Mol Biol Evol. 2004;21(11):2130–9.
2. Barrett SC, Hough J. Sexual dimorphism in flowering plants. J Exp Bot. 2013;64(1):67–82.
3. Darolti I, Wright AE, Pucholt P, Berlin S, Mank JE. Slow evolution of sex-biased genes in the reproductive tissue of the dioecious plant *Salix viminalis*. Mol Ecol. 2018;27(3):694–708.
4. Ma W-J, Veltsos P, Sermier R, Parker DJ, Perrin N. Evolutionary and developmental dynamics of sex-biased gene expression in common frogs with proto-Y chromosomes. Genome Biol. 2018;19(1):1–17.
5. Pointer MA, Harrison PW, Wright AE, Mank JE. Masculinization of gene expression is associated with exaggeration of male sexual dimorphism. PLoS Genet. 2013;9(8):e1003697.
6. Dewsbury DA. The Darwin-Bateman paradigm in historical context. Integr Comp Biol. 2005;45(5):831–7.
7. Janicke T, Häderer IK, Lajeunesse MJ, Anthes N. Darwinian sex roles confirmed across the animal Kingdom. Sci Adv. 2016;2(2):e1500983.
8. Siljestam M, Martinossi-Allibert I. Anisogamy does not always promote the evolution of mating competition traits in males. Am Nat. 2024;203(2):230–53.
9. Parker GA. The sexual cascade and the rise of pre-ejaculatory (Darwinian) sexual selection, sex roles, and sexual conflict. Cold Spring Harb Perspect Biol. 2014;6(10):a017509.
10. Lehtonen J, Parker GA. Gamete competition, gamete limitation, and the evolution of the two sexes. MHR: Basic Sci Reproductive Med. 2014;20(12):1161–8.
11. Umen J, Coelho S. Algal sex determination and the evolution of anisogamy. Annu Rev Microbiol. 2019;73:267–91.
12. Parker GA, Baker RR, Smith V. The origin and evolution of gamete dimorphism and the male-female phenomenon. J Theor Biol. 1972;36(3):529–53.
13. Cox PA, Sethian JA. Gamete motion, search, and the evolution of anisogamy, oogamy, and chemotaxis. Am Nat. 1985;125(1):74–101.
14. Levitan DR. The importance of sperm limitation to the evolution of egg size in marine invertebrates. Am Nat. 1993;141(4):517–36.
15. Cosmides LM, Tooby J. Cytoplasmic inheritance and intragenomic conflict. J Theor Biol. 1981;89(1):83–129.
16. Kodric-Brown A, Brown JH. Anisogamy, sexual selection, and the evolution and maintenance of sex. Evol Ecol. 1987;1:95–105.
17. Janicke T. Anisogamy and the Darwin–Bateman paradigm. *Evolution Letters* 2024.
18. Lehtonen J, Kokko H. Two roads to two sexes: unifying gamete competition and gamete limitation in a single model of anisogamy evolution. Behav Ecol Sociobiol. 2011;65:445–59.
19. Smith JM. The origin and maintenance of sex. In: *Group selection.* Routledge; 2017: 163–175.
20. Lipinska A, Cormier A, Luthringer R, Peters AF, Corre E, Gachon CM, Cock JM, Coelho SM. Sexual dimorphism and the evolution of sex-biased gene expression in the brown Alga ectocarpus. Mol Biol Evol. 2015;32(6):1581–97.
21. Lehtonen J, Horinouchi Y, Togashi T, Parker GA. Evolution of anisogamy in organisms with parthenogenetic gametes. Am Nat. 2021;198(3):360–78.
22. Togashi T, Nomura K, Mochizuki K, Parker GA, Horinouchi Y. An ulvophycean marine green Alga produces large parthenogenetic isogametes as predicted by the gamete dynamics model for the evolution of anisogamy. Biol Lett. 2024;20(10):20240489.
23. Constable GWA, Kokko H. Parthenogenesis and the evolution of anisogamy. Cells. 2021;10(9):2467.
24. McArthur D, Moss B. Gametogenesis and gamete structure of *Enteromorpha intestinalis* (L.) link. Brit Phycol J. 1979;14(1):43–57.
25. Melkonian M. Flagellar roots, mating structure and gametic fusion in the green Alga *Ulva lactuca* (Ulvales). J Cell Sci. 1980;46(1):149–69.
26. Miyamura S, Hori T, Nagumo T. Eyespot behavior during the fertilization of gametes in *Ulva arasakii* Chihara (Ulvophyceae, Chlorophyta). Phycol Res. 2003;51(3):143–6.
27. Smith GM. On the reproduction of some Pacific Coast species of *Ulva*. Am J Bot 1947:80–7.
28. Bråten T. The ultrastructure of fertilization and zygote formation in the green Alga *Ulva mutabilis* Føyn. J Cell Sci. 1971;9(3):621–35.
29. Mogi Y, Kagami Y, Kuwano K, Miyamura S, Nagumo T, Kawano S. Asymmetry of eyespot and mating structure positions in *Ulva Compressa* (Ulvales, Chlorophyta) revealed by a new field emission scanning electron microscopy method. J Phycol. 2008;44(5):1290–9.
30. Liu X, Blomme J, Bogaert KA, D'hondt S, Wichard T, Deforce D, Van Nieuwerburgh F, De Clerck O. Transcriptional dynamics of gametogenesis in the green seaweed *Ulva mutabilis* identifies an RWP-RK transcription factor linked to reproduction. BMC Plant Biol. 2022;22(1):19.
31. Kessler RW, Crecelius AC, Schubert US, Wichard T. In situ monitoring of molecular changes during cell differentiation processes in marine macroalgae through mass spectrometric imaging. Anal Bioanal Chem. 2017;409(20):4893–903.
32. Yang Z. PAML 4: phylogenetic analysis by maximum likelihood. Mol Biol Evol. 2007;24(8):1586–91.
33. Catalán A, Macias-Munoz A, Briscoe AD. Evolution of sex-biased gene expression and dosage compensation in the eye and brain of *Heliconius* butterflies. Mol Biol Evol. 2018;35(9):2120–34.
34. Togashi T, Bartelt JL. Evolution of anisogamy and related phenomena in marine green algae. In: *The Evolution of Anisogamy: A Fundamental Phenomenon Underlying Sexual Selection.* Edited by T Togashi, Cox P. Cambridge, UK: Cambridge Univ. Press; 2011: 194–242.
35. Løvlie A. Genetic control of division rate and morphogenesis in *Ulva mutabilis* Føyn. C R Trav Lab Carlsberg. 1964;34:77–168.
36. Nahor O, Morales-Reyes CF, Califano G, Wichard T, Golberg A, Israel Á. Flow cytometric measurements as a proxy for sporulation intensity in the cultured macroalga *Ulva* (Chlorophyta). Bot Mar. 2021;64(2):83–92.
37. Cui J, Shi J, Zhang J, Wang L, Fan S, Xu Z, Huo Y, Zhou Q, Lu Y, He P. Rapid expansion of *Ulva* blooms in the yellow Sea, China through sexual reproduction and vegetative growth. Mar Pollut Bull. 2018;130:223–8.
38. Løvlie A. Genetic control of division rate and morphogenesis in *Ulva mutabilis* Føyn. C R Trav Lab Carlsberg. 1963;34:77–168.
39. Løvlie A, Bråten T. On the division of cytoplasm and Chloroplast in the multicellular green Alga *Ulva mutabilis* Foyn. Exp Cell Res. 1968;51(1):211.
40. Stratmann J, Paputsoglu G, Oertel W. Differentiation of *Ulva mutabilis* (Chlorophyta) gametangia and gamete release are controlled by extracellular inhibitors. J Phycol. 1996;32:1009–21.
41. Jonnalagadda S, Srinivasan R. Principal components analysis based methodology to identify differentially expressed genes in time-course microarray data. BMC Bioinformatics. 2008;9(1):1–16.
42. Lahti DC, Johnson NA, Ajie BC, Otto SP, Hendry AP, Blumstein DT, Coss RG, Donohue K, Foster SA. Relaxed selection in the wild. Trends Ecol Evol. 2009;24(9):487–96.
43. Katsaros C, Weiss A, Llangos I, Theodorou I, Wichard T. Cell structure and microtubule organisation during gametogenesis of *Ulva mutabilis* Føyn (Chlorophyta). Bot Mar. 2017;60(2):123–35.
44. Kryazhimskiy S, Plotkin JB. The population genetics of dN/dS. PLoS Genet. 2008;4(12):e1000304.
45. Swanson WJ, Vacquier VD. The rapid evolution of reproductive proteins. Nat Rev Genet. 2002;3(2):137–44.

46. Kosakovsky Pond SL, Poon AF, Velazquez R, Weaver S, Hepler NL, Murrell B, Shank SD, Magalis BR, Bouvier D, Nekrutenko A. HyPhy 2.5—a customizable platform for evolutionary hypothesis testing using phylogenies. Mol Biol Evol. 2020;37(1):295–9.
47. Wertheim JO, Murrell B, Smith MD, Kosakovsky Pond SL, Scheffler K. RELAX: detecting relaxed selection in a phylogenetic framework. Mol Biol Evol. 2015;32(3):820–32.
48. Mank JE. The transcriptional architecture of phenotypic dimorphism. Nat Ecol Evol. 2017;1(1):0006.
49. Hunt BG, Ometto L, Wurm Y, Shoemaker D, Yi SV, Keller L, Goodisman MA. Relaxed selection is a precursor to the evolution of phenotypic plasticity. Proc Natl Acad Sci U S A. 2011;108(38):15936–41.
50. Togashi T, Bartelt JL, Yoshimura J, Tainaka K-i, Cox PA. Evolutionary trajectories explain the diversified evolution of isogamy and anisogamy in marine green algae. Proc Natl Acad Sci U S A. 2012;109(34):13692–7.
51. Brown RM, Johnson SC, Bold HC. Electron and phase-contrast microscopy of sexual reproduction in *Chlamydomonas Moetvusii*. J Phycol. 1968;4(2):100–20.
52. Hatchett WJ, Jueterbock AO, Kopp M, Coyer JA, Coelho SM, Hoarau G, Lipinska AP. Evolutionary dynamics of sex-biased gene expression in a young XY system: insights from the brown Alga genus *Fucus*. New Phytol. 2023;238(1):422–37.
53. Yamazaki T, Ichihara K, Suzuki R, Oshima K, Miyamura S, Kuwano K, Toyoda A, Suzuki Y, Sugano S, Hattori M. Genomic structure and evolution of the mating type locus in the green seaweed *Ulva partita*. Sci Rep. 2017;7(1):11679.
54. Provasoli L. Media and prospects for the cultivation of marine algae. In: *Cultures and Collections of Algae Proceedings of US-Japan Conference, Hakone, September 1966: 1968*. Japan Society of Plant Physiology.
55. Wichard T, Oertel W. Gametogenesis and gamete release of *Ulva mutabilis* and *Ulva lactuca* (Chlorophyta): regulatory effects and chemical characterization of the swarming inhibitor. J Phycol. 2010;46(2):248–59.
56. Le Bail A, Dittami SM, de Franco P-O, Rousvoal S, Cock MJ, Tonon T, Charrier B. Normalisation genes for expression analyses in the brown Alga model *Ectocarpus siliculosus*. BMC Mol Biol. 2008;9(1):75.
57. De Clerck O, Kao S-M, Bogaert KA, Blomme J, Foflonker F, Kwantes M, Vancaester E, Vanderstraeten L, Aydogdu E, Boesger J, et al. Insights into the evolution of multicellularity from the sea lettuce genome. Curr Biol. 2018;28(18):2921–e29332925.
58. Haas BJ, Delcher AL, Mount SM, Wortman JR, Smith RK Jr, Hannick LI, Maiti R, Ronning CM, Rusch DB, Town CD. Improving the Arabidopsis genome annotation using maximal transcript alignment assemblies. Nucleic Acids Res. 2003;31(19):5654–66.
59. Trapnell C, Roberts A, Goff L, Pertea G, Kim D, Kelley DR, Pimentel H, Salzberg SL, Rinn JL, Pachter L. Differential gene and transcript expression analysis of RNA-seq experiments with tophat and cufflinks. Nat Protoc. 2012;7(3):562–78.
60. Anders S, Pyl PT, Huber W. HTSeq—a Python framework to work with high-throughput sequencing data. Bioinformatics. 2015;31(2):166–9.
61. Robinson MD, McCarthy DJ, Smyth GK. EdgeR: a bioconductor package for differential expression analysis of digital gene expression data. Bioinformatics. 2010;26(1):139–40.
62. Flynn JM, Hubley R, Goubert C, Rosen J, Clark AG, Feschotte C, Smit AF. RepeatModeler2 for automated genomic discovery of transposable element families. Proc Natl Acad Sci U S A. 2020;117(17):9451–7.
63. Smit AF. Repeat-Masker Open-4.0. 2015, http://www.repeatmasker.org
64. Haas BJ, Salzberg SL, Zhu W, Pertea M, Allen JE, Orvis J, White O, Buell CR, Wortman JR. Automated eukaryotic gene structure annotation using evidencemodeler and the program to assemble spliced alignments. Genome Biol. 2008;9(1):1–22.
65. Hoff KJ, Lange S, Lomsadze A, Borodovsky M, Stanke M. BRAKER1: unsupervised RNA-Seq-based genome annotation with GeneMark-ET and AUGUSTUS. Bioinformatics. 2016;32(5):767–9.
66. Kovaka S, Zimin AV, Pertea GM, Razaghi R, Salzberg SL, Pertea M. Transcriptome assembly from long-read RNA-seq alignments with StringTie2. Genome Biol. 2019;20(1):1–13.
67. Keller O, Kollmar M, Stanke M, Waack S. A novel hybrid gene prediction method employing protein multiple sequence alignments. Bioinformatics. 2011;27(6):757–63.
68. Shao M, Kingsford C. Accurate assembly of transcripts through phase-preserving graph decomposition. Nat Biotechnol. 2017;35(12):1167–9.
69. Zhang X, Ye N, Liang C, Mou S, Fan X, Xu J, Xu D, Zhuang Z. De Novo sequencing and analysis of the *Ulva Linza* transcriptome to discover putative mechanisms associated with its successful colonization of coastal ecosystems. BMC Genomics. 2012;13:1–13.
70. Emms DM, Kelly S. OrthoFinder: phylogenetic orthology inference for comparative genomics. Genome Biol. 2019;20:1–14.
71. Abascal F, Zardoya R, Telford MJ. TranslatorX: multiple alignment of nucleotide sequences guided by amino acid translations. Nucleic Acids Res. 2010;38(suppl2):W7–13.
72. Stamatakis A. RAxML version 8: a tool for phylogenetic analysis and post-analysis of large phylogenies. Bioinformatics. 2014;30(9):1312–3.
73. Alvarez-Carretero S, Kapli P, Yang Z. Beginner's guide on the use of PAML to detect positive selection. Mol Biol Evol. 2023;40(4):msad041.

Publisher's note